Journal of Achievements in Materials and Manufacturing Engineering
VOLUME 49
ISSUE 1
November
2011

Microstructure, magnetic and elastic properties of electrodeposited Cu+Ni nanocomposites coatings

A. Chrobak [a,*], M. Kubisztal [b], J. Kubisztal [b], E. Chrobak [c], G. Haneczok [b]
[a] Institute of Physics, Silesian University,
ul. Uniwersytecka 4, 40-007 Katowice, Poland
[b] Institute of Materials Science, Silesian University,
ul. Bankowa 12, 40-007 Katowice, Poland
[c] Department of Organic Chemistry, Medical University of Silesia,
ul. Jagiellońska 4, 41-200 Sosnowiec, Poland
* Corresponding author: E-mail address: artur.chrobak@us.edu.pl

Received 03.09.2011; published in revised form 01.11.2011

Properties

ABSTRACT

Purpose: The paper presents systematic studies of fabrication and properties of Cu+Ni nanocomposite coatings obtained by electrodeposition technique. Special attention is paid to establish the influence of fabrication conditions and microstructure of the coating material on its magnetic and elastic properties.
Design/methodology/approach: The results were obtained by applying electrochemical impedance spectroscopy (EIS, PARSTAT 2273, roughness factor), magnetization versus temperature measurements (2<T<300 K, field 0.5 T), vibrating reed technique (Young's modulus) and scanning electron microscope (Hitachi S-4200(4)).
Findings: Magnetization curves M(T) show a superparamagnetic effect at T<50 K which depends on dispersion of magnetic particles in a nonmagnetic matrix. This effect is proportional to the field H_S required to saturate the magnetization curve M(H). So, the determination of the H_S gives information about the dispersion of magnetic particles in a nonmagnetic matrix. It was shown that the observed decrease of the apparent Young's modulus due to an increase of coating roughness can be well described by exponential function different for nano-sized and micro-sized Ni powder.
Research limitations/implications: The method of fabrication of Cu+Ni nanocomposite coatings and the examination methods of elastic and magnetic properties of these kinds of materials can be used in many fields in materials science.
Practical implications: The proposed method of evaluating of dispersion degree of magnetic nano-sized powder in nonmagnetic matrix can be applied in many problems of magnetic nanocomposite materials.
Originality/value: The paper presents application of a non-destructive approach to determination of elastic and magnetic properties of coating materials. A new method of evaluating a dispersion factor of nano-sized magnetic particle embedded into non-magnetic matrix is proposed.
Keywords: Coating materials; Elastic properties; Magnetic properties; Dispersion factor; Roughness factor

Reference to this paper should be given in the following way:
A. Chrobak, M. Kubisztal, J. Kubisztal, E. Chrobak, G. Haneczok, Microstructure, magnetic and elastic properties of Cu+Ni nanocomposites coatings obtained by applying electrodeposition technique, Journal of Achievements in Materials and Manufacturing Engineering 49/1 (2011) 17-26.

1. Introduction

Metal matrix based composite coatings obtained by electroplating method are known in materials science and engineering industry as materials with specific functional characteristics that are mostly unobtainable for bulk substrate or non-composite metal coatings e.g. self-lubrication, good corrosion resistance or wear resistance [1-3]. On the list of different applications one can find corrosion protective coatings, luminescence coatings, reducing surface friction coatings and also electromagnetic shields [4-8]. It is known that mechanical susceptibility of any coating to an applied external stress is one of the most important factors allowing to evaluating applicability of these kinds of materials. Indeed, as it was shown in [9-12] elastic properties of coating materials (i.e. Young's modulus) are coupled with coating adhesion to a given substrate. Such coupling can be described by the so-called apparent Young's modulus which can be directly used to study the ability of application of a given coating material.

Irrespective of the application aspect the nanocomposite coatings are also used as model materials for studying some basic problems in materials science. A good example are magnetic nanoparticles in nonmagnetic matrix which allows studying properties of the so-called diluted magnetism i.e. superparamagnetism or spin glass like states [7,13-15]. One of the most effective methods of fabrication of nanocomposite coatings is electrolytic deposition for which the physical properties of the obtained material strongly depend on parameters of the applied procedure (i.e. current density, bath agitation, magnetic field and/or cathode movement) [4,5,16-18].

It is clear that to obtain electrolytic coatings with a given properties it is necessary to establish the proper mechanism of the composite coating electroplating. In this context, some quantitative and qualitative models are presented and discussed in literature [4,19,20]. Nevertheless, considering the complexity of the problem the additional studies are still required. It seems that special attention has to be drawn to the fact that at given plating conditions one can obtain the composite coatings with a relatively high degree of surface development which can be quantitatively determine via measuring of the so-called roughness factor R_f. Such composite coatings are frequently tested as electrode materials in hydrogen or oxygen evolution reaction [21,22]. However, increase in coating surface development results also in a drastic change in mechanical susceptibility of the composite what may impede its industrial application.

The aim of the present paper is to study both elastic and magnetic properties of the Cu+Ni nanocomposite coatings obtained by applying the electrolytic deposition method. In such studies one of the most important problems is dispersion of magnetic nanoparticles showing a tendency to agglomeration due to their dipolar magnetic interaction. Different modifications of the classical electrodeposition procedures have been studied carefully. For an estimation of magnetic nanoparticles dispersion degree in Cu based nanocomposite coatings a new approach has been proposed. The second examined problem relates to correlations between surface morphology of the electrolytic composite coating Cu+Ni with dispersed Ni nanopowder particles (e.g. qualitatively described by roughness factor) and elastic properties (the apparent Young's modulus). In this study the following techniques have been used: i) electrochemical impedance spectroscopy [21] and ii) vibrating reed technique [9]. The obtained results were discussed in relation to the Cu+Ni composite coatings with embedded micro size Ni particles.

2. Experimental

Magnetic Cu+Ni nanocomposite coatings on Cu substrate (EN CW004A) were obtained by applying electrolytic deposition using the electrolyte consisting of $CuSO_4$ $5H_2O$ (150 g/l) and H_2SO_4 (10 g/l) to which Ni powder in amount of C_e ranging from 0.1 to 20 mg/ml was added (Ni powder grain size up to 100 nm or 3-4 μm produced by Aldrich). Directly before each electrodeposition the substrate was chemically etched by immersion in the solution of: H_2SO_4 - 10 vol.%, HNO_3 - 3 vol.%, HCl - 1 vol.%, H_2O - 86 vol.%. The examined samples in a form of rectangular plate with an active surface of about 1-4 cm^2 were obtained at room temperature using a galvanostatic method in two different configurations:

i) the perpendicular configuration (PC) with vibrating anode (frequency 20 kHz) in which current direction is vertical as shown in Fig.1a; in this case three different procedures (denoted as PC1, PC2 and PCG) have been used: a) PC1 with C_e in the range from 5 to 20 mg/ml, b) PC2 with C_e in the range from 0.1 to 2 mg/ml with fixed coating thickness (as a constant coating thickness is required for studying some physical properties) and c) PCG with C_e in the range from 5 to 20 mg/ml and addition of glycerol (25 vol. %) in order to increase the electrolyte viscosity,
ii) the horizontal configuration (HC) with mechanical stirring in which current direction is horizontal as shown in Fig 1b ($5 \le C_e \le 20$ mg/ml).

It is important to note, that in the applied fabrication procedure with the sample-anode configuration shown in Fig. 1a the transport of Ni powder particles towards the cathode substrate is provided not only by external potential difference but also by gravitational force that ensures increasing concentration of Ni in the area of the cathode surface. However, if the concentration of Ni on the cathode surface area is too high one can expect the deposition blocking effect which may result in coating thickness lower than predicted based on the charge transport relation. In order to prevent such behavior in PC configuration we impose the plating cycle (with different current density and C_e values) that consists of three successive steps: i) agitation of the electrolyte i.e. the anode vibrations are switched on for 10 seconds, ii) the anode vibrations are switched off for 5 seconds and iii) the deposition current (1 – 100 mA/cm^2) is on for 120 seconds. These three steps were repeated until the deposition time t_d reaches the assumed value. Before and after the deposition each sample was weighted with the precision of 10^{-5}g and based of the weight increase the coating thickness was evaluated. The Ni content in Cu matrix C_{Ni} was determined by applying magnetic method via measuring the total sample magnetic moment (magnetic balance technique).

Magnetic measurements i.e. magnetization M versus temperature (in the range 2-300 K, magnetic field $\mu_0 H$=0.5 T) and magnetization curves $M(H)$ ($0<\mu_0 H<7$ T) were carried out by applying Physical Properties Measurements System (PPMS) of Quantum Design.

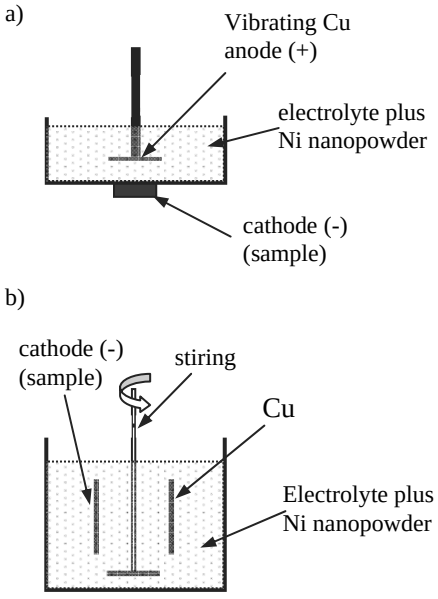

Fig. 1. Two configurations used in electrodeposition of Cu+Ni nanocomposite a) the perpendicular configuration (PC), and b) the horizontal configuration (HC)

Elastic properties of the Cu+Ni nanocomposites coatings were examined by applying the so-called vibrating reed technique in clamped-free configuration (for detail see [9]). As it was shown in [9-12] the dynamic response of the coating material is described by the so-called apparent Young's modulus $E_a=\gamma^2 E_f$ (where γ is the adhesion coefficient and E_f is the Young's modulus of the coating material) which can be determined via measuring the frequency of free vibrations of sample subjected to small external stress usually corresponding to a strain of the order of 10^{-5}. The experimental procedure consists of two steps: i) measurement of the free flexural vibration frequency f_s of the Cu substrate and ii) measurement of the free flexural vibration frequency f_c of the substrate coated by applying the plating procedure described above. According to [9, 10] $E_a=\gamma^2 E_f$ can be determined using the equation:

$$\frac{f_c^2 - f_s^2}{f_s^2} = \frac{d_f}{d_s}\left(\frac{3E_a}{E_s} - \frac{\rho_f}{\rho_s}\right) \quad (1)$$

where E_s is the Young's modulus of the substrate, d is the thickness, ρ is the density and subscripts s and f stand for substrate and coated substrate, respectively. It is interesting to note, that adhesion coefficient γ in equation (1) introduced by Wuttig in [23] is defined by taking into account a discontinuity in the elastic energy transfer from the substrate to the coating during its flexural vibrations. In this approach the adhesion coefficient γ may take the values in the range 0-1 where γ=1 means that coating is perfectly adhered to the substrate while γ=0 means no adherence. In this respect both quantities Young's modulus E_f and the adhesion coefficient γ should be considered as the elastic properties of the coating material. This issue is discussed in detail in [9] where also some applications in materials science of the vibrating reed technique are shown.

The surface morphology of the obtained coatings was investigated by means of electrochemical impedance spectroscopy (EIS, PARSTAT 2273) and scanning electron microscope (SEM, Hitachi S-4200(4)). EIS measurements were performed at open circuit potential in the frequency range from 10 kHz to 100 mHz after immersion of the studied coatings in naturally aerated 0.5 wt.% H_2SO_4 for 1 h. The approximation of the impedance data was performed using a ladder model with electrical equivalent circuit predicting two time constants i.e. low-frequency time constant related to the kinetics of the corrosion processes and high-frequency time constant related to the development of the electrode surface [1,21,24,25]. According to this approach the roughness factor R_f that describes the coating surface development can be calculated from the ratio of C_i/C_r where C_i represents the capacitance of the investigated composite coating determined from high frequency part of the impedance spectrum (subscript i numbers the successive composite coatings with different content of Ni powder) and C_r stands for the reference capacitance of the Cu substrate. So, for Cu substrate we have arbitrary R_f=1 and for coatings with higher surface development R_f factor takes correspondingly higher values.

3. Results and discussion

The obtained results with regard to Cu+Ni nanocomposite coating technology as well as magnetic and elastic properties of the fabricated samples are presented and discussed in the next sections of this paragraph.

3.1. Electrodeposition mechanism and microstructure of Cu+Ni nanocomposite coatings

Fig. 2 shows C_{Ni} (Ni concentration in Cu+Ni nanocomposite coating) and coating thickness plotted versus current density j for the procedure PC1 with C_e=10 mg/ml and deposition time t_d=30 min. One can see that C_{Ni} increases linearly with current density while the coating thickness initially is constant and for j≥40 mA/cm^2 strongly decreases. This means that the highest value of C_{Ni} (≈20 wt.%) corresponds to a relatively high current density (≈80 mA/cm^2) and rather thin Cu coating (≈1μm). The decrease of coating thickness for high current density (at constant t_d) can be explained by accumulation of Ni powder from the electrolyte on the sample surface. This means that for higher current density certain fraction of Cu is deposited on the powder surface and blocks the Cu ions transport to the electrode surface.

In order to avoid the Cu deposition blocking effect observed in Fig. 2 the sample fabrication procedure was modified in two ways:

i) by adding to electrolyte 25 % of glycerol in order to increase the electrolyte viscosity (PCG procedure) and
ii) by reducing the content of Ni powder in electrolyte C_e (PC2 procedure).

Fig. 3 shows C_{Ni} and coating thickness plotted versus current density j for the procedure PCG with C_e=10 mg/ml and deposition

time t_d=30 min. One can see that an addition of about 25 vol. % of glycerol to the electrolyte (PCG) does not eliminate the blocking effect for current densities j > 30 mA. In this case the value of C_{Ni} of about 5 wt. % can be obtained for j=60 mA/cm^2 and the coating thickness of about 5 μm. Fig. 4 shows C_{Ni} plotted versus current density j for the procedure PC2 with different C_e (0.1, 1 and 2 mg/ml) and constant coating thickness d_f=30 μm. In these experiments in order to obtain the coatings with given thickness at different current density i.e. j=10, 20 and 40 mA/cm^2 the electroplating process was carried out for 15, 30 and 60 cycles (see preceding section), respectively. According to this figure the Ni content embedded into Cu matrix increases with increasing C_e and for a given C_e slightly decreases with current density. The latter indicate that in this procedure the Cu deposition blocking effect does not play any role.

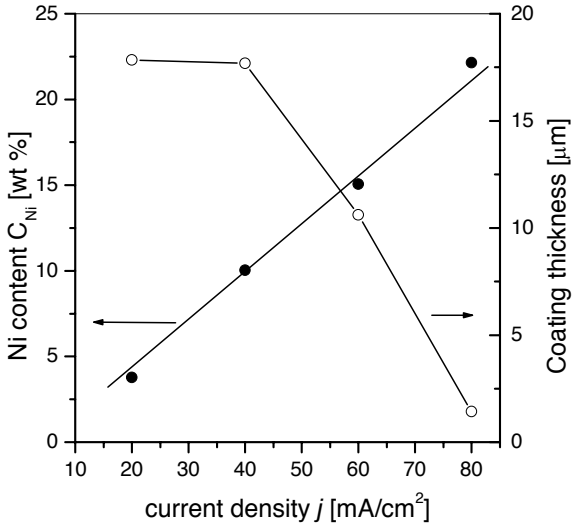

Fig. 2. Ni powder content C_{Ni} and coating thickness of electrodeposited Cu+Ni coating versus current density j for the procedure PC1 with C_e=10 mg/ml and deposition time 30 min

The results obtained by applying the HC configuration are presented in Fig. 5 where C_{Ni} and coating thickness are plotted versus current density j for C_e=10 mg/ml and the deposition time t_d=30 min (as for Figs. 2 and 3). Such results show that C_{Ni} decreases with increasing current density and Cu deposition is not hindered by the blocking effect which is in agreement with [26].

Fig. 6 shows the plot of C_{Ni} versus concentration C_e for Cu+Ni composite coatings with embedded nano-sized and micro-size Ni particles obtained at the same deposition current density j=40 mA/cm^2. It can be seen that applying micro size Ni particles a significant increase in C_{Ni} is observed in comparison with nanocomposite coatings. For example, at C_e=1 mg /ml the content of Ni in the composite coating increases from 2 wt.% to 17 wt.%.

Figs. 7a-7f show microstructures of the examined composites coatings. Figs. 7a and 7b depict two SEM images for samples obtained by applying PC1 and PCG procedures with similar C_{Ni} of about 3.7-3.8 wt. % (Figs. 7a and 7b, respectively). It is evident that an addition of glycerol into electrolyte causes a reduction of grain size of the obtained coating. The mean grain size for sample of Fig. 7a (PC1) was estimated as 8.0 μm while from Fig. 7b (PCG) as 2.0 μm. The microstructure of the composite coating obtained by applying HC procedure is similar to the one presented in Fig. 7a.

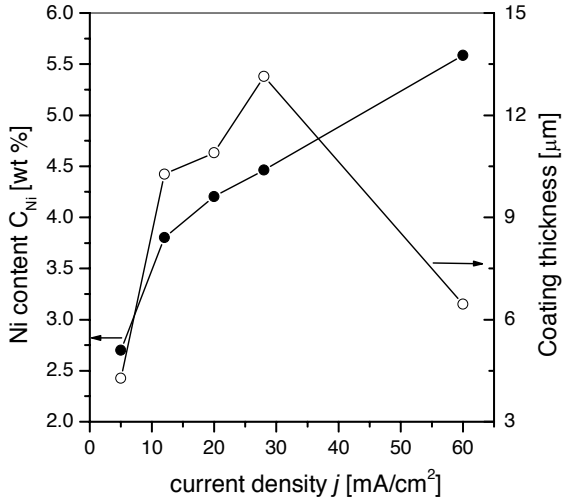

Fig. 3. Ni powder content C_{Ni} and coating thickness of electrodeposited Cu+Ni coating versus current density j for the procedure PCG with C_e=10 mg/ml and deposition time 30 min

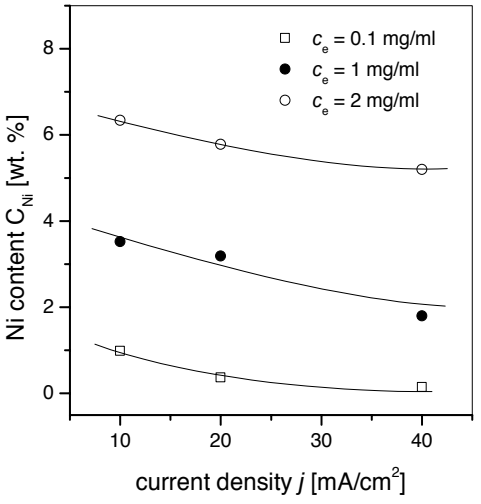

Fig. 4. Ni powder content in Cu+Ni nanocomposite coating C_{Ni} plotted versus current density j for the procedure PC2 with different C_e (0.1, 1 and 2 mg/ml) and constant coating thickness d_f=30 μm

Figs. 7c-f present SEM examinations of the coating surface morphology for PC2 procedure. The difference in surface development of Cu coating obtained at j=40 mA/cm^2 (Fig. 7c) and Cu+Ni nanocomposite coatings with comparable C_{Ni} (5.2 and 6.3

wt.%) but obtained at different current densities i.e. j=40 mA/cm^2 (Fig. 7d) and 10 mA/cm^2 (Fig. 7e) is well documented. Fig. 7f depicts a cross section of Cu+Ni composite with micro Ni powder. The surface development of the examined Cu+Ni coatings was examined via measuring the so-called roughness factor R_f using electrochemical impedance spectroscopy technique.

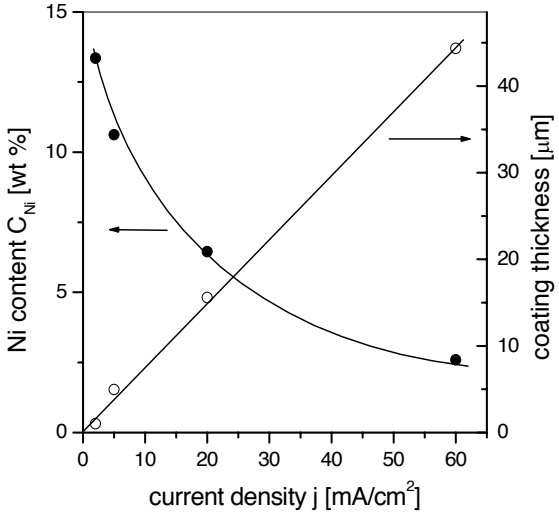

Fig. 5. Ni powder content C_{Ni} and coating thickness of electrodeposited Cu+Ni coating versus current density j for the configuration HC with C_e=10 mg/ml and deposition time 30 min

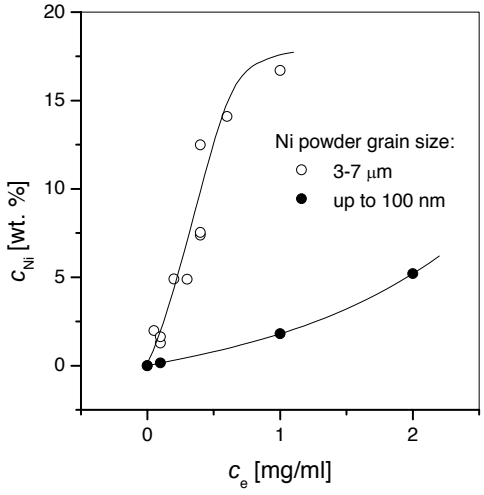

Fig. 6. Ni powder content C_{Ni} versus concentration of Ni powder in the electrolyte C_e for nano and micro size powder particles

The results are presented in Fig. 8 where R_f is plotted versus C_{Ni} for two different powder of Ni i.e. micro-sized and nano-sized. One can see that nano-sized Ni powder causes an increase of roughness factor much more effectively than the micro-sized one.

In order to explain the results presented in Figs. 2-8 it is necessary to take into consideration the mechanism of composite coating electroplating. According to the proposal of Celis et al. in [20] one can expect that Ni particles introduced to the plating solution are nearly immediately surrounded by Cu^{2+} ionic cloud forming electrically charged particles denoted as $Ni_{Cu(2+)}$. In our case such positively charged particles move towards the cathode surface under the influence of both the electric field applied in the plating process and the gravity proportional to the mass of a singular $Ni_{Cu(2+)}$ particle. Note, that $Ni_{Cu(2+)}$ particles that are in direct contact with the cathode surface for sufficiently long time (i.e. longer than time necessary for reduction of the Cu^{2+} ions) can be reduced to the inert form of Ni_{Cu}. So, the amount of individual reduction reactions of the $Ni_{Cu(2+)}$ particles on the cathode surface results in the effective incorporation of the Ni phase into the electrodeposited Cu matrix. One can state that in the first approximation it should depend on the applied deposition current density j as well as on the c_e values. In fact, the results presented in Fig. 4 show that the increase in C_e (i.e. increase in amount of $Ni_{Cu(2+)}$ particles in the suspension) gives rise to an increase in Ni particles incorporated into the copper matrix described by C_{Ni} value. However, the dependence of C_{Ni} on deposition current density j seems to be much more complex i.e. taking into account a wide range of j one can obtain the relation with characteristic maximum as reported in [20]. In a case of PC2 and HC configuration (see Figs. 4 and 5) we observe a decrease in C_{Ni} for four different concentration of the Ni powder in the plating solution. It can be explained by taking into account that the applied plating conditions assure that co-deposition of Ni particles with Cu^{2+} ions is controlled by mass transport in the suspension. If it is the case then increase in deposition current density j may result in partial desorption of the Cu^{2+} ions from the $Ni_{Cu(2+)}$ particles and/or in increase in the rate of Cu matrix deposition what gives the observed decrease in C_{Ni} value in Figs. 4 and 5.

Note, that the reduction process of a singular $Ni_{Cu(2+)}$ particle on the cathode surface results in formation of some local irregularity which in electroplating process may play a role of the privilege center. It seems that cathode electrons in this region may locally increase the hydrogen evolution reaction rate that occurs simultaneously with coating deposition process. The increased concentration of hydrogen atoms at the privilege center favours the formation of the hydrogen blisters which adjacent to the surface irregularities impede the electrolytic plating. Such effect obviously leads to the formation of the Ni_{Cu} clusters around the hydrogen blister and promotes the increase in surface development of the obtained composite coating with increasing C_{Ni} and j values. Data presented in Fig. 8 (i.e. R_f (C_{Ni})) obtained for Cu+Ni composite coatings with embedded nano and micro Ni particles and SEM micrographs in Figs. 7c, d and e confirm the interpretation presented above. Note, that the electroplating mechanism discussed above assures that Ni_{Cu} clusters deposited on the cathode substrate consist of the Ni particles surrounded by Cu film (Fig. 7f). This fact allows to state that Ni phase dispersed in the Cu matrix does not have direct contact with the substrate and consequently the adhesion of the composite coating to the Cu substrate is fully described by the adhesion of the Cu matrix i.e. does not depend on Ni content in the coating.

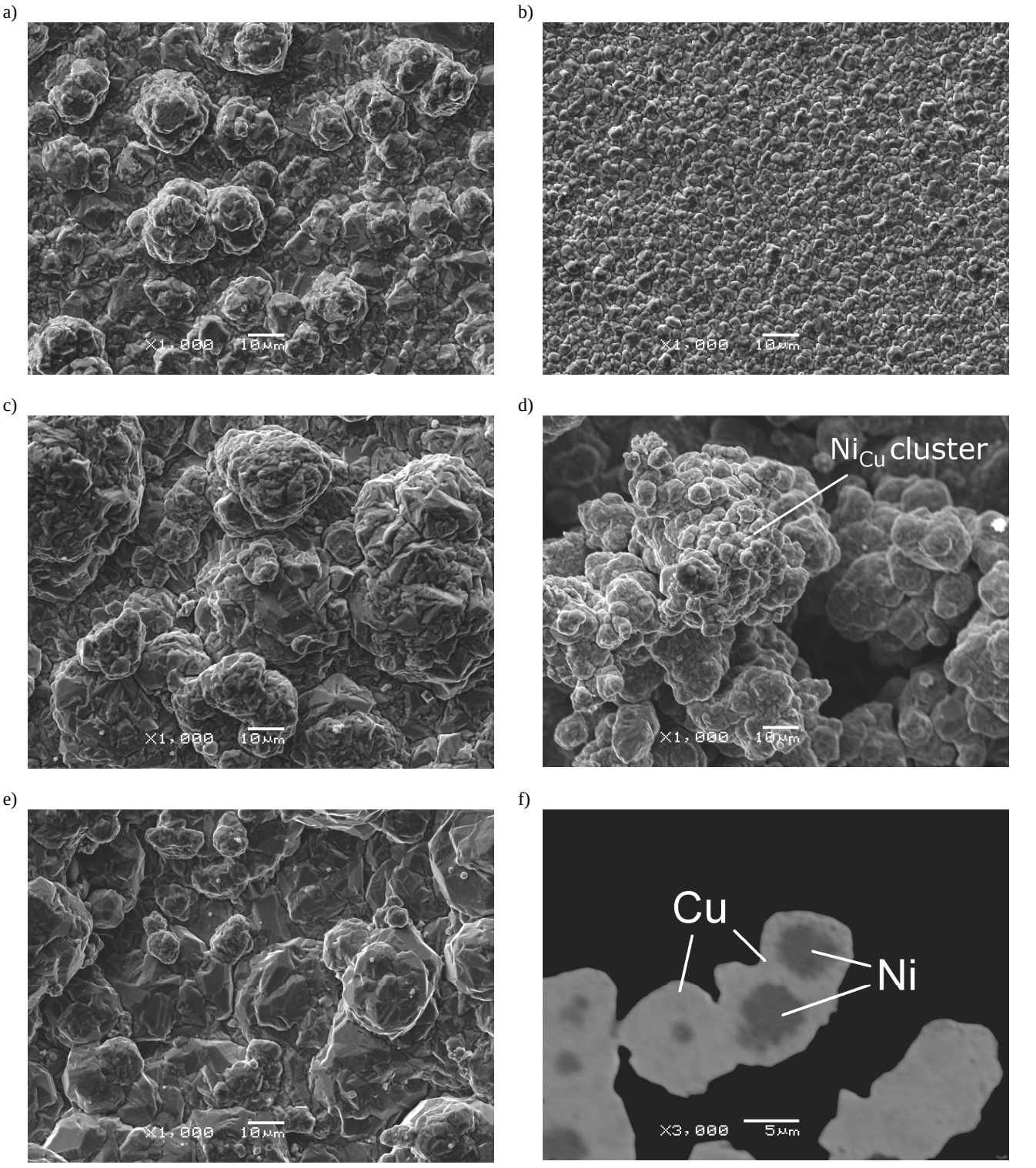

Fig. 7. Microstructure of Cu+Ni nanocomposite coating obtained by applying: a) PC1 procedure (C_{Ni}=3.8 wt.%); b) PCG procedure (C_{Ni}=3.7 wt. %); c) PC2 procedure, pure Cu, j=40 mA/cm^2, d) PC2 procedure, Cu+Ni nanocomposite, C_{Ni}=5.2 wt.%, j=40 mA/cm^2, e) PC2 procedure, Cu+Ni nanocomposite, c_m=6.3 wt.%, j=10 mA/cm^2; f) PC2 procedure, cross section for Cu+Ni composite coating (particles 3-7 μm)

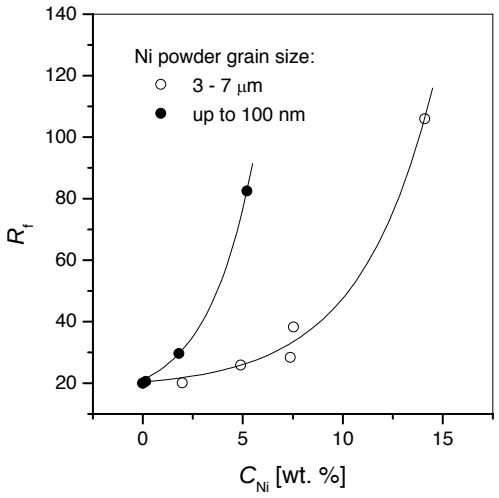

Fig. 8. Roughness factor R_f versus Ni powder content C_{Ni} embedded into Cu matrix

3.2. Magnetic properties

Fig. 9 shows for three selected samples the temperature dependence of magnetization M measured at $\mu_0 H$=0.5 T. One can see that for T>50 K a saturation effect is observed as it can be expected for a typical ferromagnetic response. At lower temperatures i.e. for T<50 K an abrupt increase of magnetization is observed

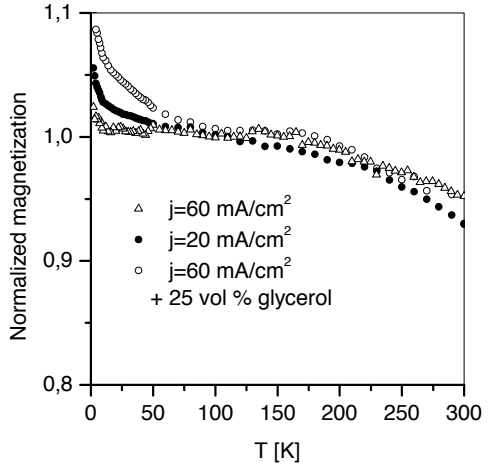

Fig. 9. Normalized magnetization in saturation versus temperature for Cu+Ni nanocomposite obtained in different conditions

Such behavior is typical for superparamagnetic material for which the Curie law is expected to be fulfilled. Indeed, for noninteracting magnetic particles the temperature dependence of magnetization is described by the Langevin function and at low temperatures due to a reduction of thermal energy the magnetization should strongly increase. Note, the magnetization of Cu+Ni nanocomposite coatings consists of two components: i) the ferromagnetic one which saturates at about 150 K connected with relatively large Ni powder grains practically acting as bulk Ni and ii) the superparamagnetic one which is observed at T<50 K related to rather small (probably mono-domains) well dispersed in Cu matrix powder grains forming a noninteracting magnetic system. Let notice that the observed superparamagnetic effect can be quantitatively described by a dimensionless factor defined as:

$$SP = \frac{M(2K) - M(150K)}{M(150K)} \qquad (2)$$

which strongly depends on sample fabrication procedure. In fact, for different procedures the dispersion of Ni powder grains in Cu matrix is expected to be different. If so, the SP factor may be considered as a measure of magnetic nanoparticles dispersion in nonmagnetic matrix because it represents the component of magnetization related to a well disperse fine noninteracting Ni nanograins.

Fig. 10 shows $M(H)$ curves measured at temperature 300 K for the same samples as presented in Fig. 9. Note, different Cu+Ni nanocomposite coatings saturate at different magnetic filed. The samples with higher SP factor require lower magnetic field H_S to reach the saturation state. Such behavior can be easily understood if Ni powder in Cu matrix is partially agglomerated. Indeed, due to dipolar interaction between magnetic nanoparticles the demagnetization factor in Ni agglomerates increases and it makes the magnetic saturation much more difficult. If this argumentation is correct the SP factor should be proportional to H_S because the both quantities reflect the Ni particles dispersion degree. The plot of SP versus H_S is shown in Fig. 11 where different points were obtained by applying different procedure of sample preparation (labeled in the figure). A linear correlation ensures that the above explanation is correct and the SP factor as well as the H_S field can be treated as a parameter proportional to the dispersion of magnetic particles in nonmagnetic matrix.

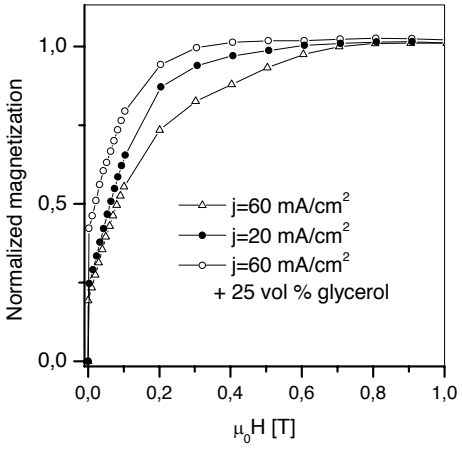

Fig. 10. Magnetization $\mu_0 M$ versus magnetic field $\mu_0 H$ for Cu+Ni coating obtained in different conditions

In order to standardize the SP factor as the dispersion parameter additional magnetic measurements were carried out for

sample prepared by a polymerization of methyl methacrylate (PMMA) with addition of 10 wt. % of Ni nano-sized powder. In order to obtain as perfect as possibly powder dispersion during the polymerization an ultrasonic bath agitation was applied. For such sample we have obtained: SP_{PMMA}=19.3 and $\mu_0 H_S$=0.20 T. Let notice that for Ni powder content of 10 wt.% perfectly dispersed the magnetic response should be roughly the same as for one small piece of Ni. The value of $\mu_0 H_S$ (measured by means of the same magnetometer) for a micro-sized Ni grain equals 0.19 T. Assuming that for the PMMA+Ni sample the dispersion factor corresponds to 100 % one can define a relative dispersion factor as $DF=SP/SP_{PMMA}$ and quantitatively present the dispersion of Ni powder in Cu+Ni nanocomposite coatings in percentage scale as shown in Fig. 11.

It is evident that for the same sample preparation procedure the dispersion factor is higher for lower values of C_{Ni}. One can conclude that the addition of glycerol to electrolyte or a significant reduction of C_e improves the powder dispersion. For example for comparable C_{Ni} values (3.8 wt % and 3.7 wt %) the addition of 25 vol % of glycerol causes an increase of DF factor from 27 % to 74 %. Approximately the same DF value corresponds to a 5-times reduction of C_e. It can be seen that PCG and PC2 procedures give at least qualitatively much more dispersed Ni particles embedded into Cu matrix in relation to the PC1 or HC procedure.

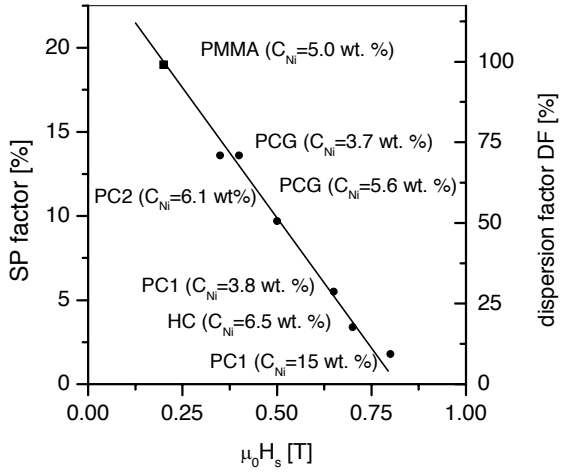

Fig. 11. Degree of dispersion of Ni powder in Cu+Ni nanocomposite calculated as relative intensity of superpara-magnetic effect (see Fig. 9; 100 % corresponds to polymethyl methacrylate + Ni powder) versus magnetic field $\mu_0 H_S$ required for magnetic saturation.

3.3. Elastic properties

The apparent Young's modulus E_a determined for the examined Cu+Ni nanocomposite samples is presented in Fig. 12 where E_a versus C_{Ni} is plotted for samples obtained by applying the procedure PC2 (coating thickness d_f=30 μm). It can be seen that E_a decreases with increasing C_{Ni} and for higher current densities j the decrease is more significant. It can be seen that for C_{Ni} of about 5 wt.% the increase in deposition current density j from 10 to 40 mA/cm^2 results in the decrease in apparent Young's modulus E_a from 135 to 90 GPa. Note also, that in the case of composite coatings obtained at j=40 mA/cm^2 the increase in C_{Ni} up to 5 wt.% corresponds to the decrease in E_a of about 35 %.

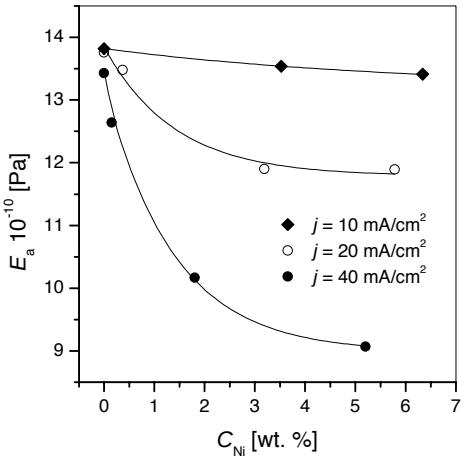

Fig. 12. Apparent Young's modulus E_a (see equation (1)) of Cu+Ni nanocomposite coatings versus C_{Ni} - content of Ni particles embedded into Cu matrix for different deposition current density j (coating thickness d_f=30 μm, procedure PC2).

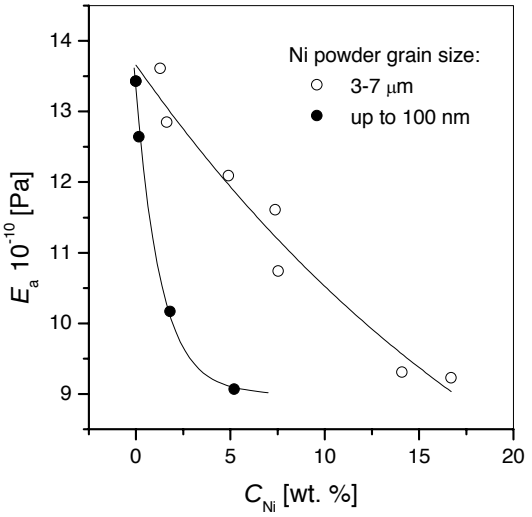

Fig. 13. Apparent Young's modulus versus C_{Ni} - content of Ni particles (nano-sized and micro-sized) embedded into Cu matrix

It is reasonably to assume that a change in coating structure should be correlated with a change in coating elastic properties i.e. an increase in C_{Ni} and/or j gives rise to the decrease of the apparent Young's modulus E_a as it was presented in Figs. 12 and 13. Note, that the electroplating mechanism discussed in the preceding section assures that Ni_{Cu} clusters deposited on the cathode substrate consist of the Ni particles surrounded by Cu film (see Fig. 7d). This fact allows to state that Ni phase dispersed

in the Cu matrix does not have direct contact with the substrate and consequently the adhesion of the composite coating to the Cu substrate is fully described by the adhesion of the Cu matrix i.e. does not depend on Ni content in the coating. Taking this fact into consideration one can conclude that the data presented in Figs. 12 and 13 show directly a change of the Young's modulus E_f with the current density j, C_{Ni} and Ni powder particle size, respectively. This conclusion is correct as long as the adhesion coefficient γ is constant. It may be that γ differs from one (see the comment below equation (1)) and in this case Figs. 12 and 13 show a relative change of the Young's modulus E_f of the coating material. Nevertheless, it has to be emphasized that elastic properties of the coating materials are properly described by the co-called apparent Young's modulus E_a, as it was discussed in [2,9-12].

In the case of Cu+Ni composite coatings with co-deposited micro size Ni powder particles (see Fig.6) one can state that contribution of the individual Ni particle to the entire content of the Ni phase introduced into the Cu matrix is significantly higher than in the case of the applied nanopowder. So, despite of the fact that for a given concentration C_e the amount of individual Ni particles in the plating solution has to be significantly lower for larger particles one can state that application of micro size Ni particles allows to obtain higher content of Ni phase in the composite coating. Note also, that in the case of micro Ni powder the mean distance between privileges centers formed onto the substrate surface is increased. It should promote the hydrogen desorption from the substrate surface and facilitate deposition of the Cu matrix. If it is correct than we should obtain composite coatings with less developed surface (i.e. lower R_f factor) and higher elastic properties in comparison with the Cu+Ni nanocomposite coatings, what is in agreement with the data presented in Figs. 8 and 13.

Mathematical analysis of the data presented in Figs. 12 and 13 shows that the experimental points can be well described by an exponential function in the form: $E_a=A\exp(-\alpha\ c_m)+B$ where B stands for E_a determined at Ni wt. % approaching infinity, A (in Pa) and α (in 1/wt.%) are constants describing the decrease rate of E_a. It means that the data of Figs. 12 and 13 in logarithmic scale should correlate in a straight line with general equation:

$$\ln(E_a - B) = -\alpha \cdot c_m + \ln A \qquad (3)$$

where: α is the slope of the straight line and ln$A$ is the intercept. The corresponding straight lines are presented in Fig. 14. One can see that all experimental points correlate in two straight lines - one for nanopowder (independently on the applied deposition current density) with $\alpha=(7\pm1)\ 10^{-1}$ [1/wt.%] and the second one for micro powder with $\alpha=(5.0\pm0.5)\ 10^{-2}$ [1/wt.%].

It has to be stressed that the parameter α for nano-sized Ni powder is more than one order of magnitude higher than for the micro sized Ni powder. The above discussion and the results presented in Fig. 14 allow advancing a hypothesis that the nature of coatings surface development formed during electroplating of metal-matrix composite depends only on the powder particle size used in experiments. It also determines the decrease rate of the Young's modulus due to an increase of coating roughness factor (two lines in Fig. 14)

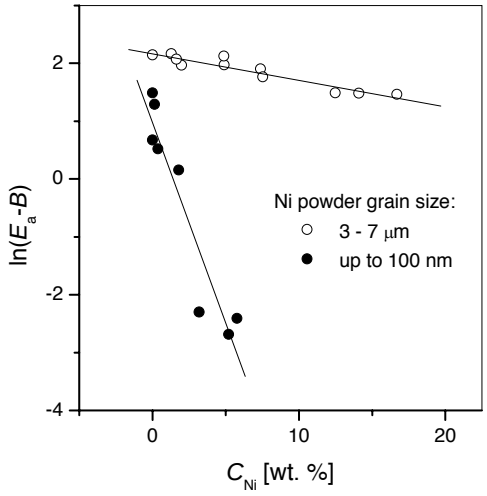

Fig. 14. Plot of ln(E_a-B) versus C_{Ni} (for details see equation (2)) for nano-sized and micro-sized Ni powder.

4. Concluding remarks

Studies presented in the paper show that magnetic Cu+Ni nanocomposite coatings can be obtained by applying the electrolytic deposition method based on a standard electrolyte and current densities in the range 1-100 mA/cm^2. In the case of the PC1 procedure (Fig. 1a) C_{Ni} increases linearly with current density while the coating thickness decreases for higher values of j (Fig. 2). This effect is connected with accumulation of Ni powder on sample surface which blocks the Cu ions transport to the electrode (sample). Using this method one can obtain Cu+Ni nanocomposite with C_{Ni} up to 20 wt.%. An addition of 25 vol % of glycerol to the electrolyte (PCG procedure) causes a reduction of mean grain size of the examined nanocomposite (about 4 times) and essentially reduces a tendency to agglomeration of magnetic particles in Cu matrix. The latter could be quantitatively measured based on measurements of magnetic properties of the material examined. It was shown that magnetization measured versus temperature shows at T<50 K a superparamagnetic behavior which depends on dispersion of magnetic particles in a nonmagnetic matrix (Fig. 9). Moreover, it was demonstrated that magnetic field H_S required to saturation of magnetization curves $M(H)$ is sensitive to agglomeration of Ni particles (Fig. 10) and is correlated with the supperparamagnetic effect (Fig. 11). This means that magnetization measurements and determination of the H_S field give information about the dispersion of magnetic particles in a nonmagnetic matrix. It was shown that the Cu+Ni nanocomposite coatings show a well developed surface with roughness factor R_f of about 80 in relation to the Cu substrate (R_f=1). A decrease in Ni particle size from micro to nanoscale results in an increase of the coating surface development (increase of the R_f from 20 to 80) and in a strong decrease in the apparent Young's modulus (from about 120 GPa to 90 GPa for C_{Ni} of about 5 wt.%). It was proposed that the mechanism of the composite coating electroplating process should take into consideration the formation of Ni_{Cu} clusters on the cathode substrate surface. This mechanism explains qualitatively the

observed increase in the coating roughness factor and in consequence a decrease of the apparent Young's modulus of the examined composite coatings. The observed decrease of the apparent Young's modulus due to an increase of coating surface development can be well described by an exponential function for which the parameter α (see equation (3)) is more than one order of magnitude higher for the nanopowder than for the micro Ni powder.

Acknowledgements

This work was supported by the Polish Ministry of Science and Higher Education under grant No. N507 317336.

References

[1] M. Lekka, G. Zendron, C. Zanella, A. Lanzutti, L. Fedrizzi, P.L. Bonora, Corrosion properties of micro- and nanocomposite copper matrix coatings produced from a copper pyrophosphate bath under pulse current, Surface and Coatings Technology 205 (2011) 3438-3447.

[2] M. Kubisztal, J. Kubisztal, A. Chrobak, G. Haneczok, A. Budniok, J. Rasek, Elastic properties of Ni and Ni+Mo coatings electrodeposited on stainless steel substrate, Surface and Coatings Technology 202 (2008) 2292-2296.

[3] A. Robin, J.L. Rosa, M.B. Silva, Electrodeposition and characterization of Cu–Nb composite coatings Surface and Coatings Technology 205 (2010) 2152-2159.

[4] M. Musiani, Electrodeposition of composites: an expanding subject in electrochemical materials science, Electrochimica Acta 45 (2000) 3397-3402.

[5] Wun-Hsing Lee, Sen-Cheh Tang, Kung-Cheng Chung, Effects of direct current and pulse-plating on the co-deposition of nickel and nanometer diamond powder, Surface and Coating Technology 120-121 (1999) 607-611.

[6] J. Steinach, H. Ferkel, Nanostructured Ni-Al_2O_3 films prepared by DC and pulsed DC electroplating, Scripta Materialia 44 (2001) 1813-1816.

[7] H. Chiriac, A.E. Moga, C. Gherasim, N. Lupu, Synthesis and Characterization of Fe-W and Ni-W Composite Coatings, Romanian Journal of Information Science and Technology 11 (2008) 123-132.

[8] A. Chrobak, A. Kaleta, P. Kwapuliński, M. Kubisztal, G. Haneczok, Magnetic shielding effectiveness of iron-based amorphous alloys and nanocrystalline composites, Proceedings of the International Conference on Soft Magnetic Materials, SMM'20, IEEE Transactions on Magnetics, Kos, 2011.

[9] M. Kubisztal, A. Chrobak, G. Haneczok, Non-destructive method of determination of elastic properties and adhesion coefficient of different coating materials, Journal of Achievements in Materials and Manufacturing Engineering 43/2 (2010) 634-643.

[10] M. Kubisztal, J. Kubisztal, A. Chrobak, G. Haneczok, Young's modulus and adhesion coefficient of amorphous Ni-P coatings on a metal substrate, Journal of Adhesion Science and Technology 21 (2007) 1009-1019.

[11] M. Kubisztal, G. Haneczok, A. Chrobak, B. Rams, D. Miara, J. Rasek, Elastic properties of epoxy system coatings on aluminum substrate, Surface and Coatings Technology 204 (2009) 120-124.

[12] A. Chrobak, M. Kubisztal, J. Kubisztal, G. Haneczok, Adhesion coefficient and elastic properties of composite coatings on metallic substrate, Surface and Coatings Technology 204 (2010) 2077-2080.

[13] A. Chrobak, B. Kotur, T. Mika, G. Haneczok, Effect of Gd and Fe doping on magnetic properties of $Al_{87}Y_5Ni_8$ amorphous alloy, Journal of Magnetism and Magnetic Materials 321 (2009) 2767–2771.

[14] A. Chrobak, A. Bajorek, G. Chełkowska, G. Haneczok, M. Kwiecień, Magnetic properties and magnetocaloric effect of $Gd(Ni_{1-x}Fe_x)_3$ crystalline compound and powder Physica Status Solidi A 206 (2009) 731-737.

[15] Xiaochun Li, Zhiwei Li, Nano-sized Si_3N_4 reinforced NiFe nanocomposites by electroplating, Materials Science and Engineering A 358 (2003) 107-113.

[16] Luisa Peraldo Bicelli, Benedetto Bozzini, Claudio Mele, Lucia D'Urzo, Corrosion Behavior of Titanium and Nickel-based Alloys in HCl and HCl + H_2S Environments, International Journal of Electrochemical Science 3 (2008) 356-408.

[17] Qiuyuan Feng, Tingju Li, Zhongtao Zhang, Jian Zhang, Mei Liu Junze Jin, Preparation of nanostructured Ni/Al_2O_3 composite coatings in high magnetic field, Surface and Coating Technology 201 (2007) 6247-6252.

[18] D. Thieming, R. Lange, A. Bund, Influence of pulse plating parameters on the electrocodeposition of matrix metal nanocomposites, Electrochimica Acta 52 (2007) 7362-7371.

[19] C.T.J. Low, R.G.A. Wills, F.C. Walsh, Electrodeposition of composite coatings containing nanoparticles in a metal deposit, Surface and Coating Technology 201 (2006) 371-383.

[20] J.P. Celis, J.R. Roos, C. Buelens, J. Fransaer, Mechanism of electrolytic composite plating: survey and trends, Transactions of the Institute of Metal Finishing 69 (1991) 133-139.

[21] J. Kubisztal, A. Budniok, A. Lasia, Study of the hydrogen evolution reaction on nickel-based composite coatings containing molybdenum powder, International Journal of Hydrogen Energy 32 (2007) 1211-1218.

[22] J. Kubisztal, A. Budniok, Study of the oxygen evolution reaction on nickel-based composite coatings in alkaline media, International Journal of Hydrogen Energy 33 (2008) 4488-4494.

[23] Q. Su, S.Z. Hua, M. Wuttig, Nondestructive dynamic evaluation of thin NiTi film adhesion, Journal of Adhesion Science and Technology 8 (1994) 625-633.

[24] R.K. Shervedani, A. Lasia, Studies of the hydrogen Evolution Reaction on Ni-P electrodes, Journal of the Electrochemical Society 144 (1997) 3214-3219.

[25] F. Wen, C. Xie, S. Cai, Y. Gui, Electrochemical behaviour of copper/LDPE composites in the simulated uterine solution, Electrochimica Acta 51 (2006) 5606-5611.

[26] I. Gurrappa, L. Binder, Electrodeposition of nanostructured coatings and their characterization a review, Science and Technology of Advanced Materials 9 (2008) 043001.